Electronic Supplementary Material (ESI) for Physical Chemistry Chemical Physics.

Supporting Information

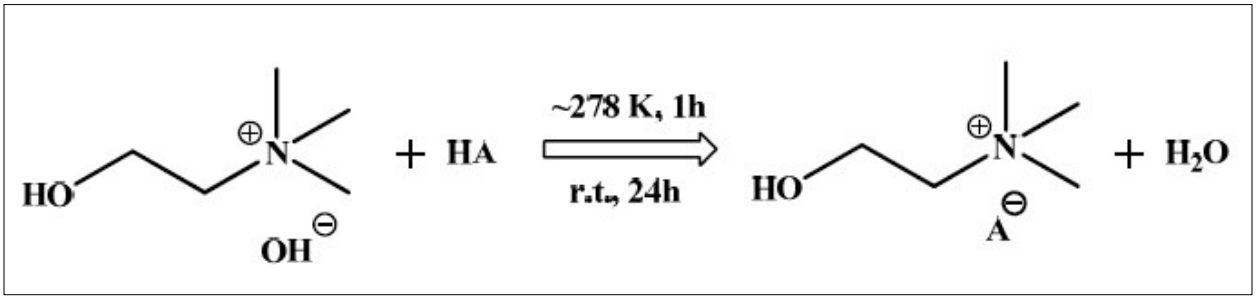

Scheme 1. Synthesis scheme of aprotic cholinium carboxylate ionic liquids.

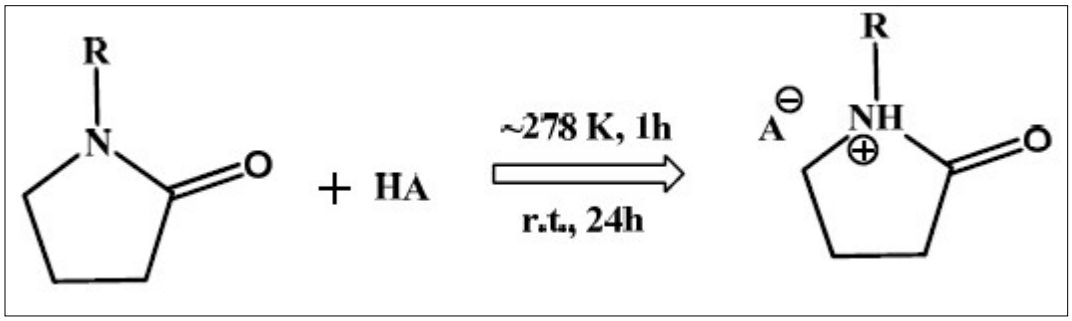

Scheme 2. Synthesis scheme of protic *N*-methyl-2-pyrrolidonium carboxylate ionic liquids.

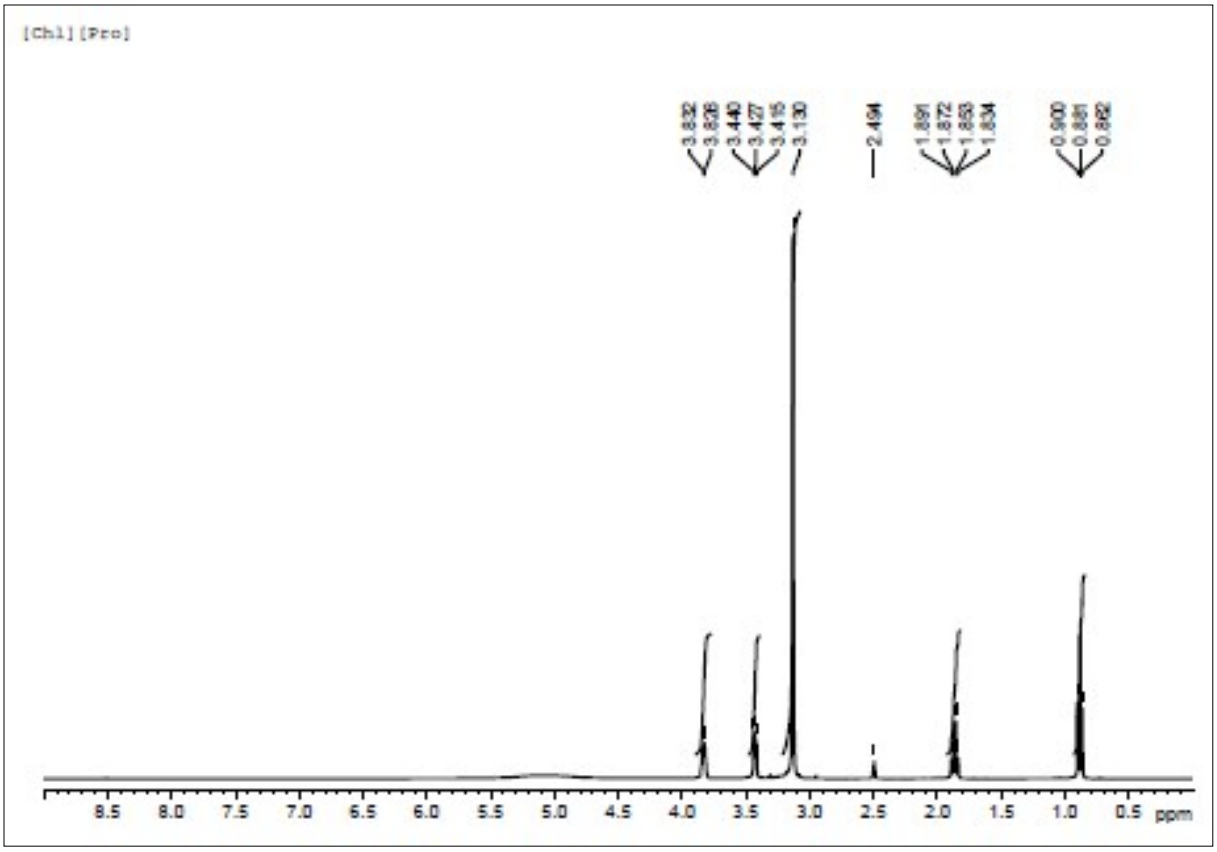

Figure S1. ^{1}H NMR of cholinium propionate, [Chl][Pro].

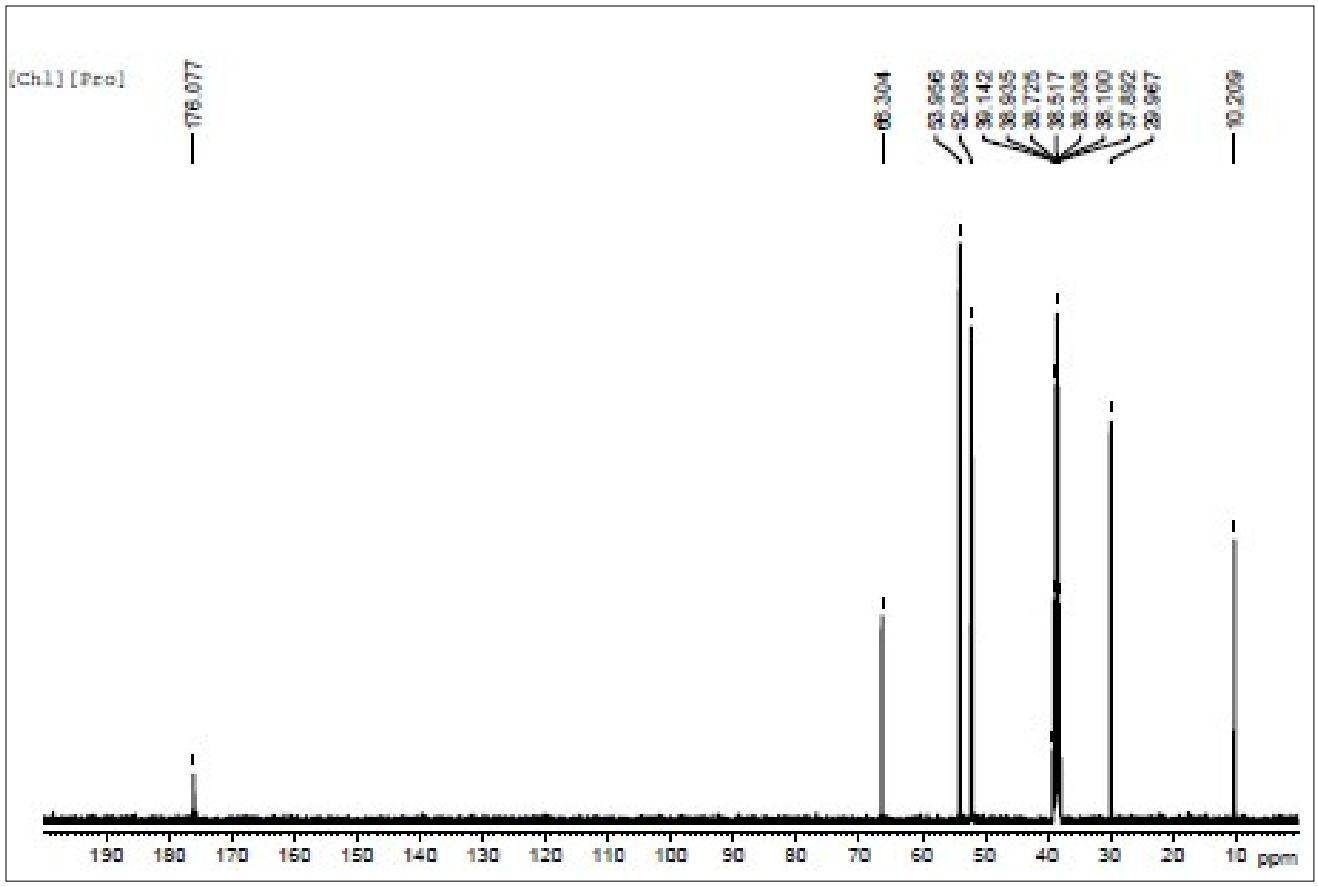

Figure S2. ^{13}C NMR of cholinium propionate, [Chl][Pro].

For [Chl][Pro], deuterated DMSO (DMSO-d_6) was used as solvent and the peak positions were at; ^{1}H-NMR (500 MHz, DMSO-d_6) [Chl][Pro]: δ (ppm) = 0.89 (t, 3H); 1.89 (q, 2H); 3.14 (s, 9H); 3.43 (t, 2H); 3.84 (s, 2H).

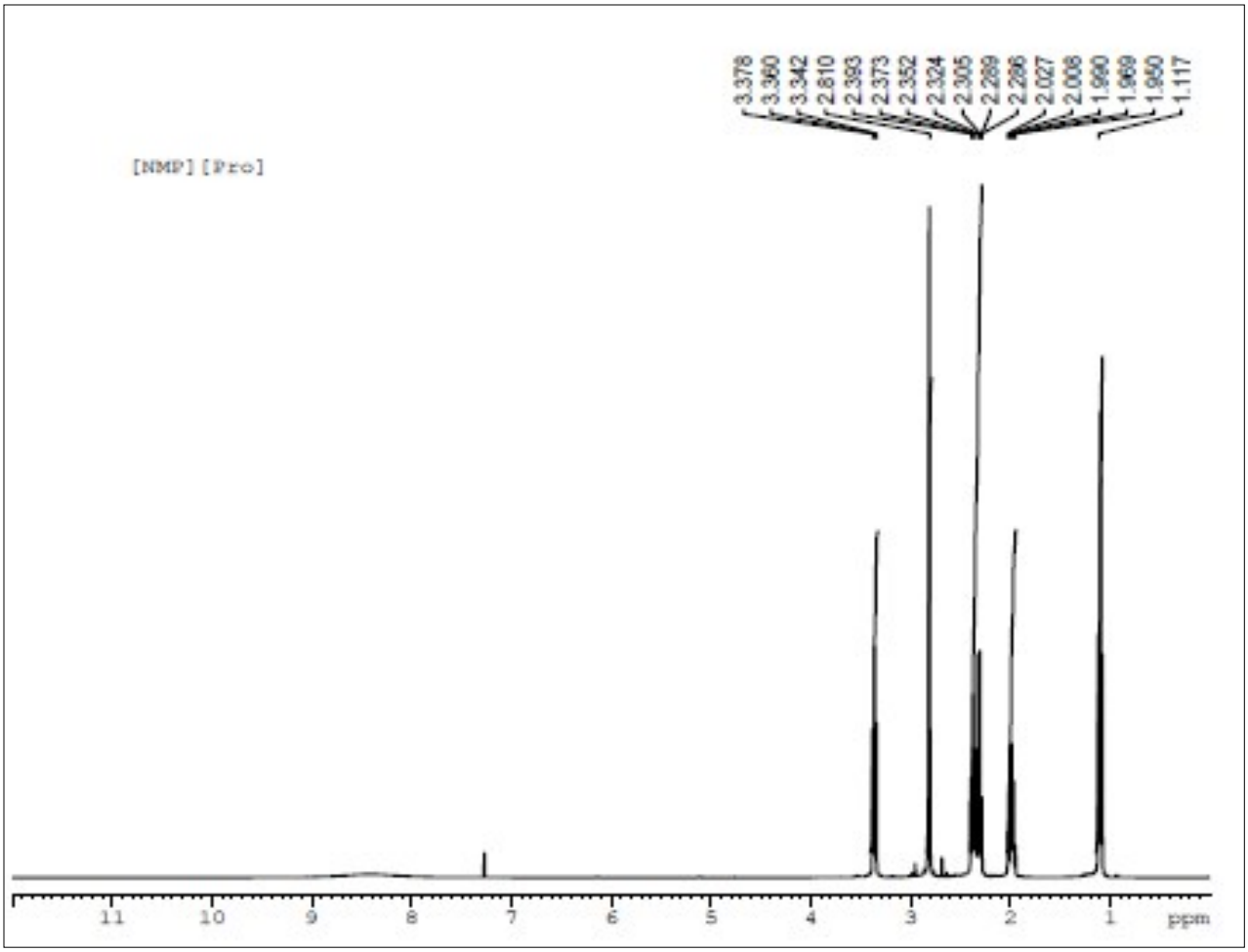

Figure S3. ^{1}H NMR of *N*-methyl-2-pyrrolidonium propionate, [NMP][Pro].

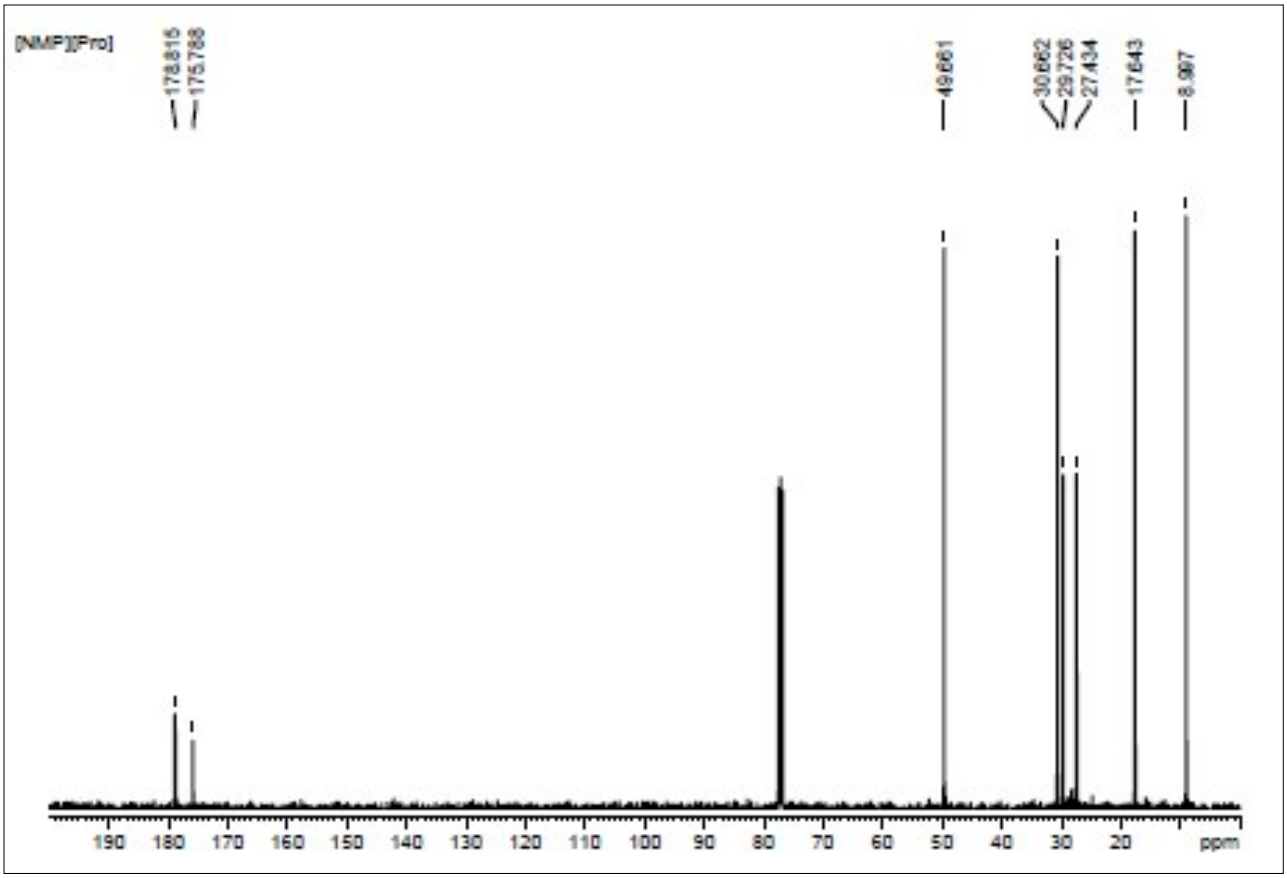

Figure S4. ^{13}C NMR of *N*-methyl-2-pyrrolidonium propionate, [NMP][Pro].

For [NMP][Pro], $CDCl_3$ was used as solvent and the peak positions were at; ^{1}H-NMR (500 MHz, $CDCl_3$) [NMP][Pro]: δ (ppm) = 1.10 (t, 3H); 2.01 (m, 2H); 2.29 (m, 2H); 2.37 (t, 2H); 2.83 (s, 3H); 3.42 (t, 2H); and 6.1 (broad NH^+).

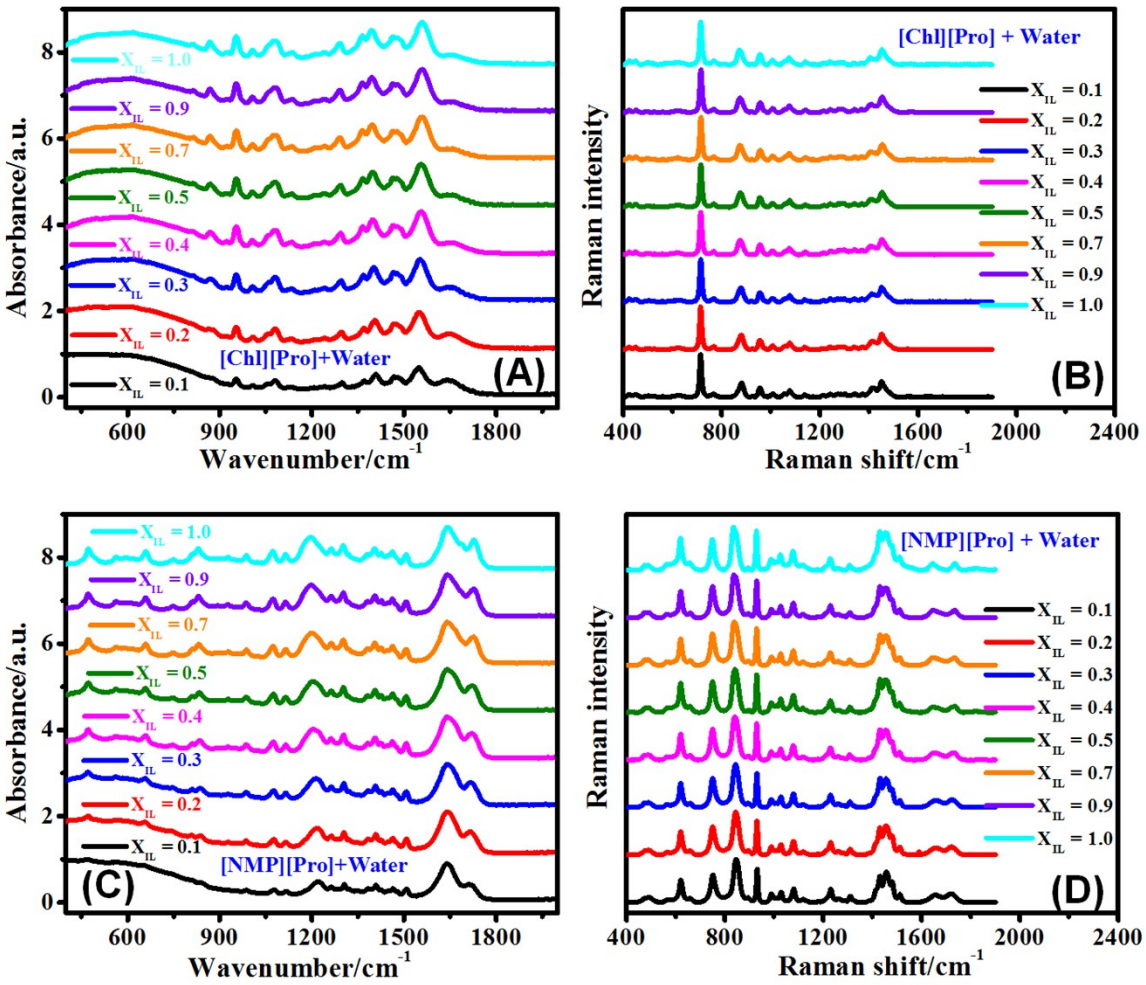

Figure S5. IR and Raman spectra of [Chl][Pro] and [NMP][Pro] ILs and their aqueous mixtures.

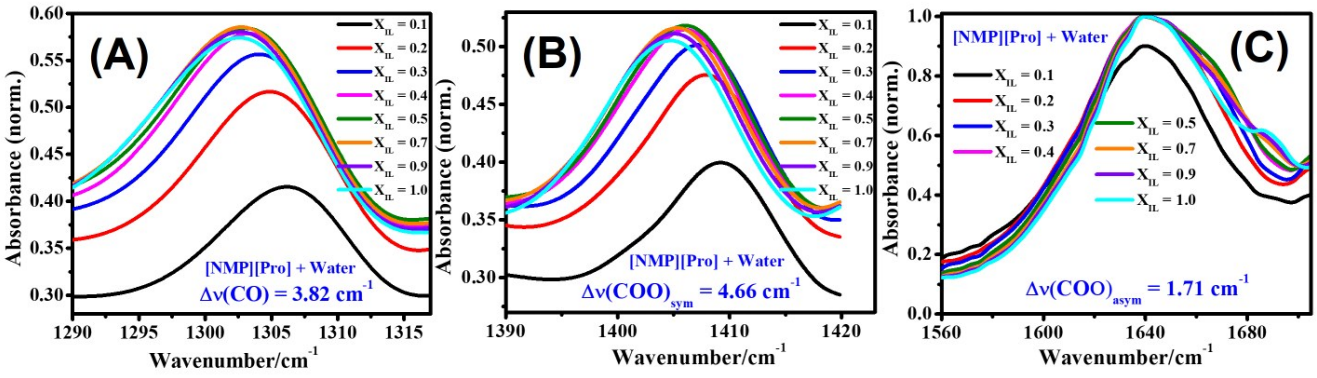

Figure S6. IR spectra of [NMP][Pro] IL at selected vibrational region.

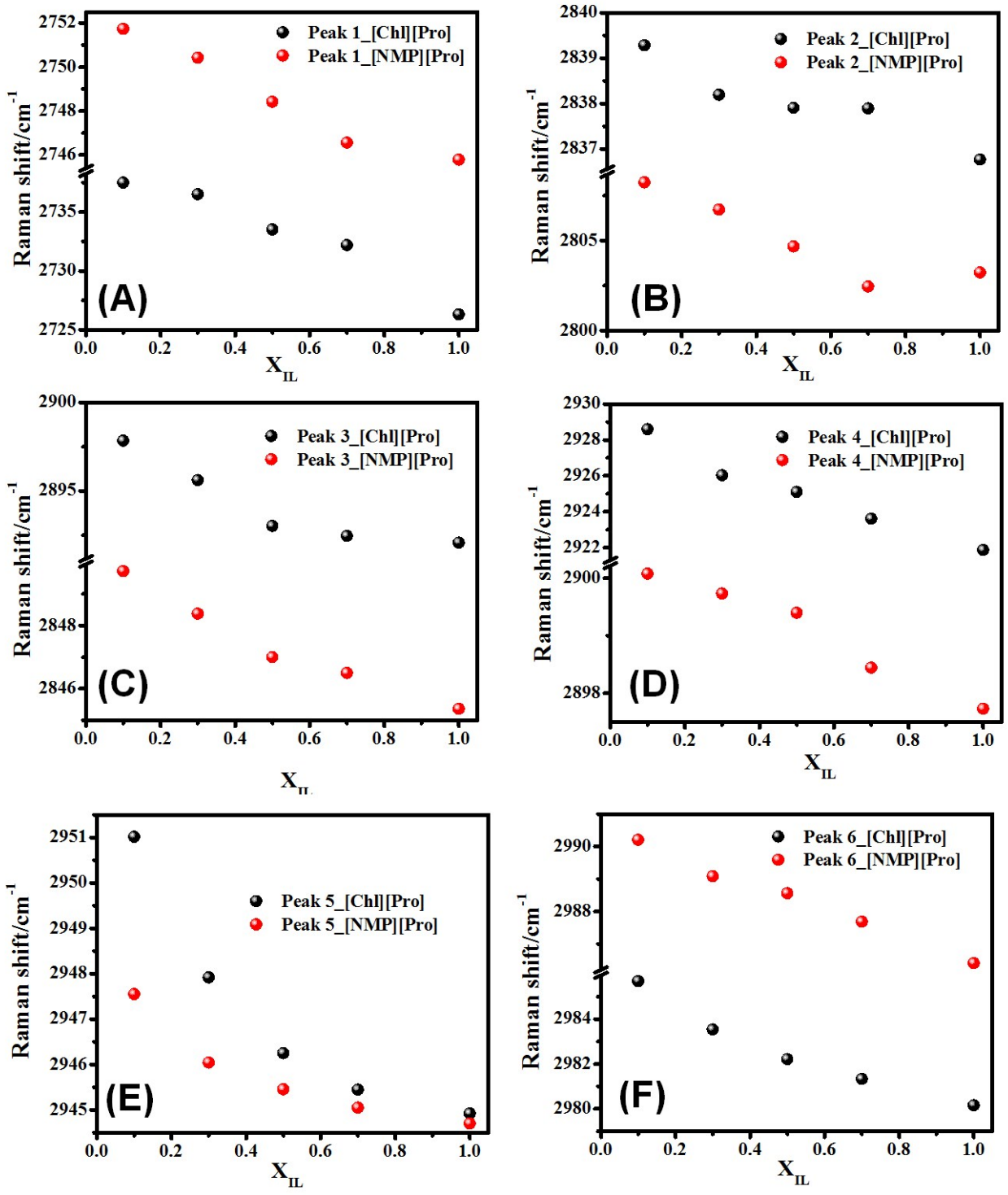

Figure S7. Change in Raman shift of deconvoluted C-H stretching frequencies as a function of IL concentration for [Chl][Pro] and [NMP][Pro] ILs.

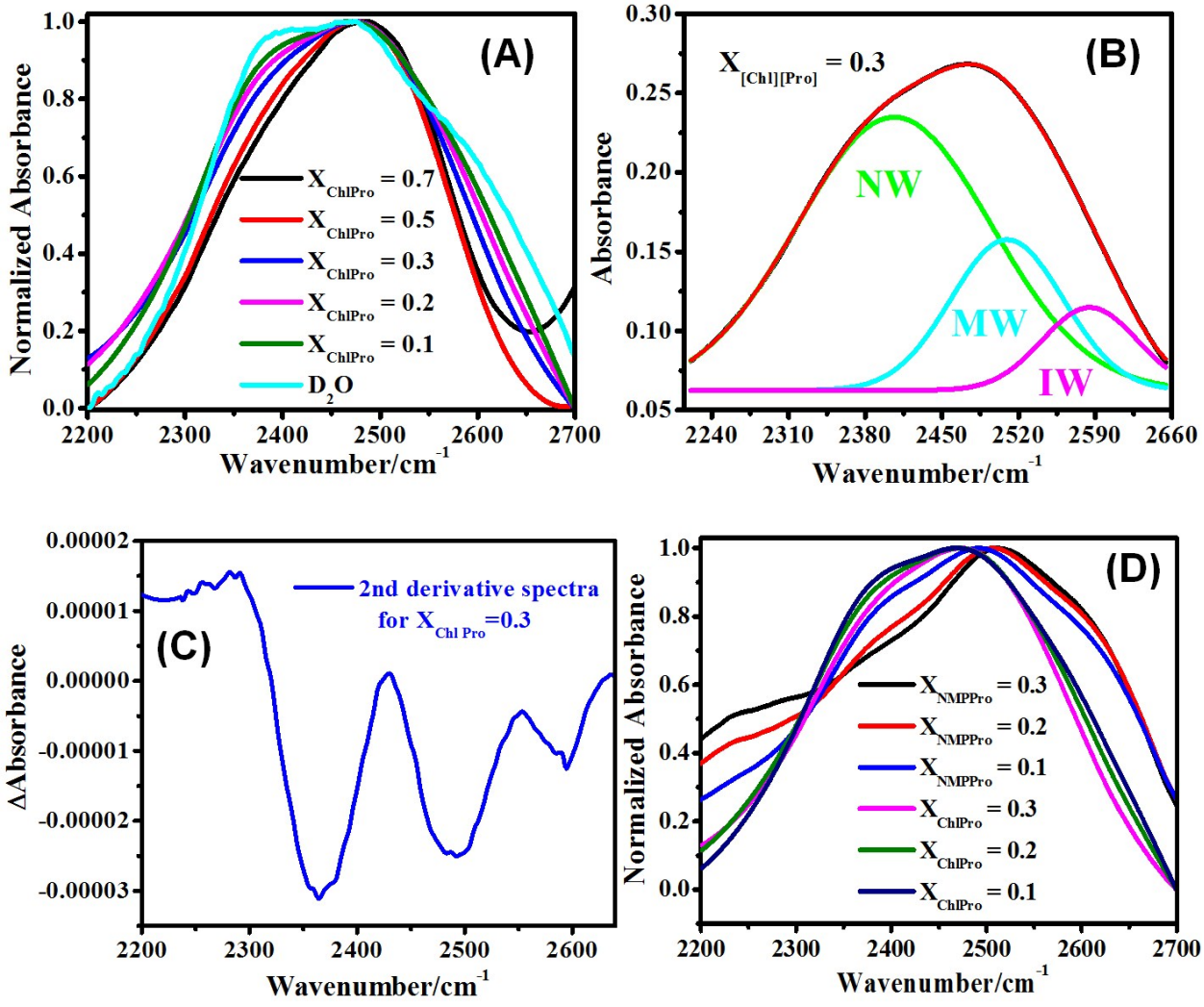

Figure S8. (A) Raman spectra at O-D region for [Chl][Pro]/D_2O mixture at different x_{IL} and neat D_2O; (B) Deconvoluted spectra and (C) 2nd derivative of ν_{OD} band for [Chl][Pro]/D_2O mixture at fixed x_{IL} of 0.3; (D) Comparative Raman spectra at O-D region for [Chl][Pro] or [NMP][Pro]/D_2O mixture at different x_{IL}.

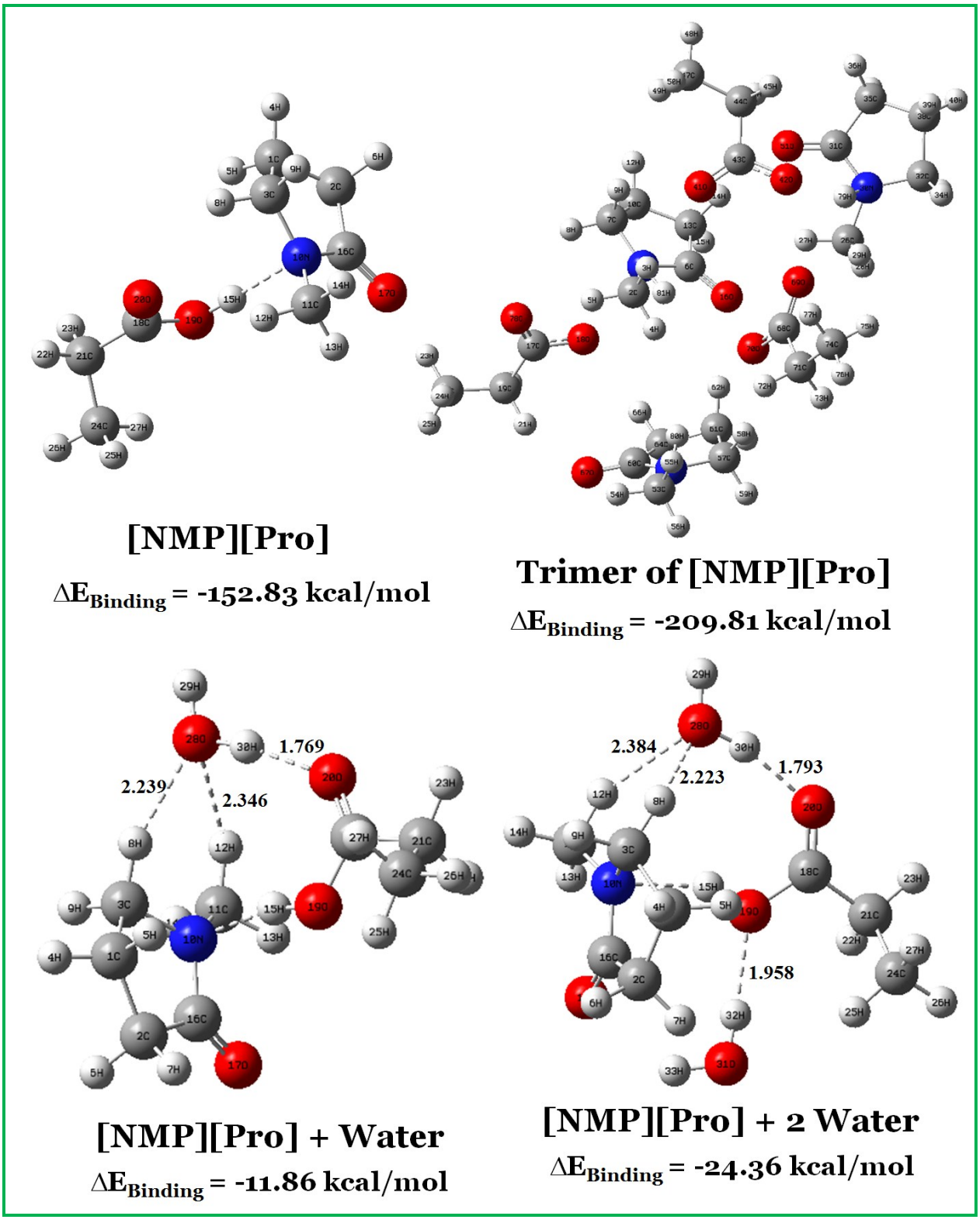

Figure S9. The most stable configurations of [NMP][Pro] ion pair and its trimer along with their complex with water, calculated at the B3LYP/6-311G theoretical level. The H-bonds are denoted

by dashed lines, and the corresponding distances are labeled in Å. The binding energies are represented under each configuration in kcal mol^{-1}.

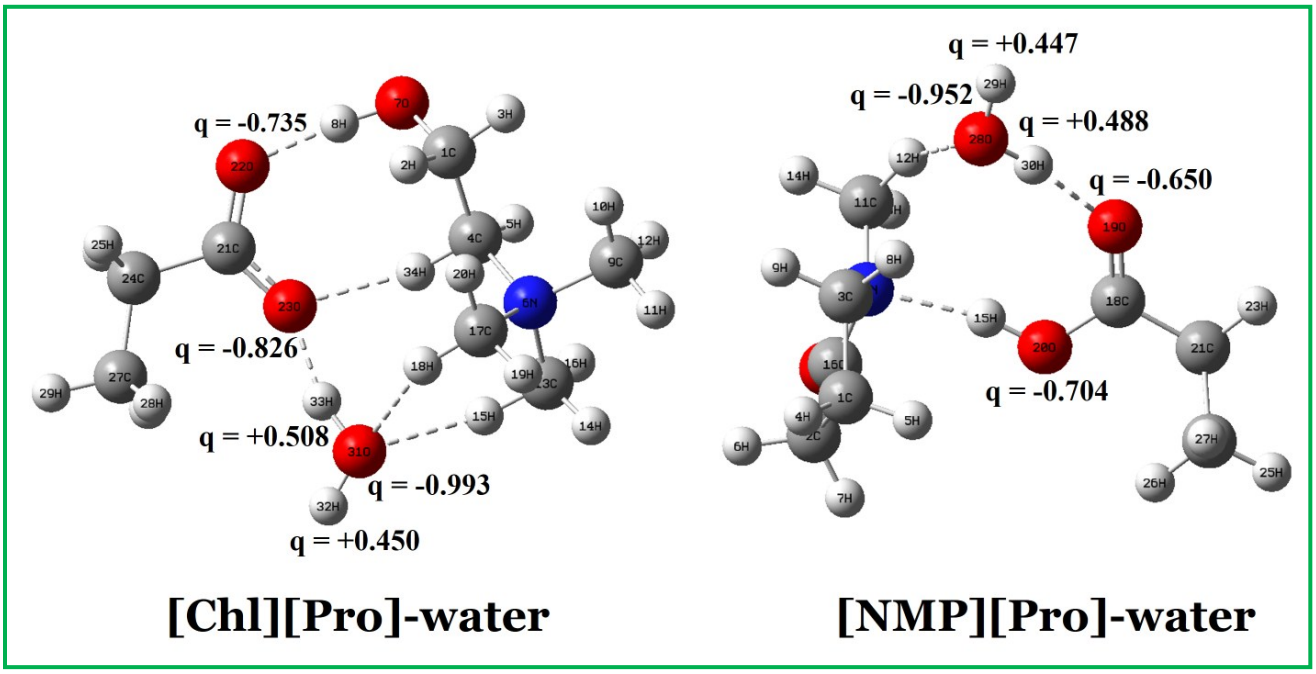

Figure S10. NBO charges of H and O atoms involved in H-bonds in [Chl][Pro]-H_2O and [NMP][Pro]-H_2O complexes.

Table S1. Second-order perturbation energy [*E*(2)] and the interacting orbitals for the water with cation and anion interactions within the IL and IL-water systems.

Donar-Acceptor Orbitals Interactions	*E*(2) (kcal/mol)
[NMP][Pro]	
LP(1)O19 → BD*(1)N10-H15	8.97
LP(2)O19 → BD*(1)N10-H15	71.78
LP(1)O20 → BD*(1)C3-H8	2.35
LP(2)O20 → BD*(1)C3-H8	2.93
LP(2)O20 → BD*(1)C11-H12	1.27
[Chl][Pro]	
LP(1)O23 → BD*(1)O8-H9	7.05
LP(2)O23 → BD*(1)O8-H9	13.14
LP(1)O24 → BD*(1)C18-H21	4.36
LP(2)O24 → BD*(1)C18-H21	6.05
LP(2)O24 → BD*(1)C1-H2	1.45
[NMP][Pro]+1W	
Anion-water	
LP(1)O19 → BD*(1)O28-H30	6.73
LP(2)O19 → BD*(1)O28-H30	8.13
Cation-water	
LP(1)O28 → BD*(1)C3-H8	1.32
LP(1)O28 → BD*(1)C11-H12	0.60
LP(2)O28 → BD*(1)C3-H8	0.96
LP(2)O28 → BD*(1)C11-H12	1.23
[Chl][Pro]+1W	
Anion-water	
LP(1)O23 → BD*(1)O31-H33	14.39
LP(2)O23 → BD*(1)O31-H33	21.36
Cation-water	
LP(1)O31 → BD*(1)C17-H18	3.20
LP(1)O31 → BD*(1)C13-H15	0.34
LP(2)O31 → BD*(1)C17-H18	1.24
LP(2)O31 → BD*(1)C13-H15	5.21

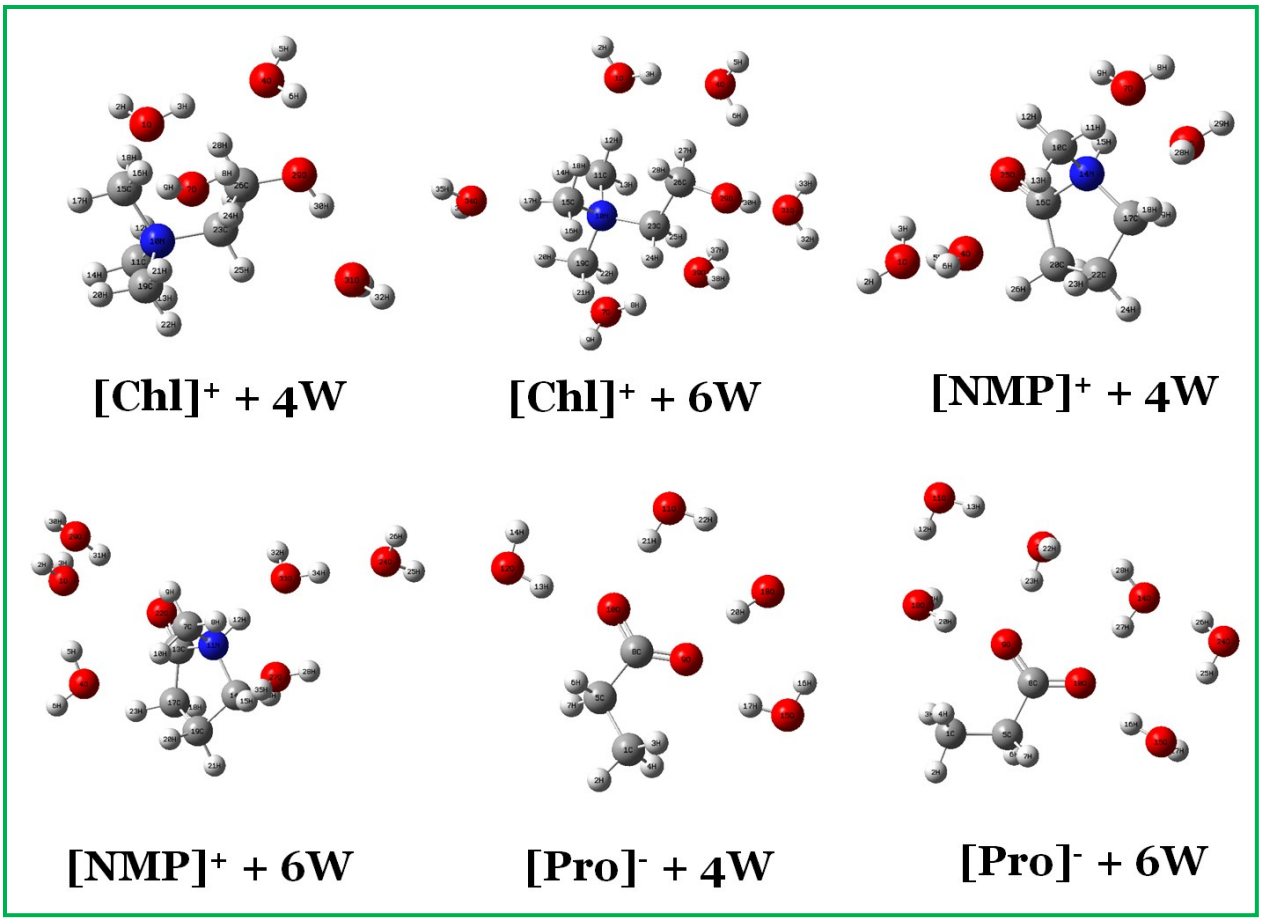

Figure S11. Optimized geometries of $[Chl]^{+}$-$(H_2O)_n$, $[NMP]^{+}$-$(H_2O)_n$ and $[Pro]^{-}$-$(H_2O)_n$ clusters, calculated at the RHF/aug-cc-pVDZ level of theory.

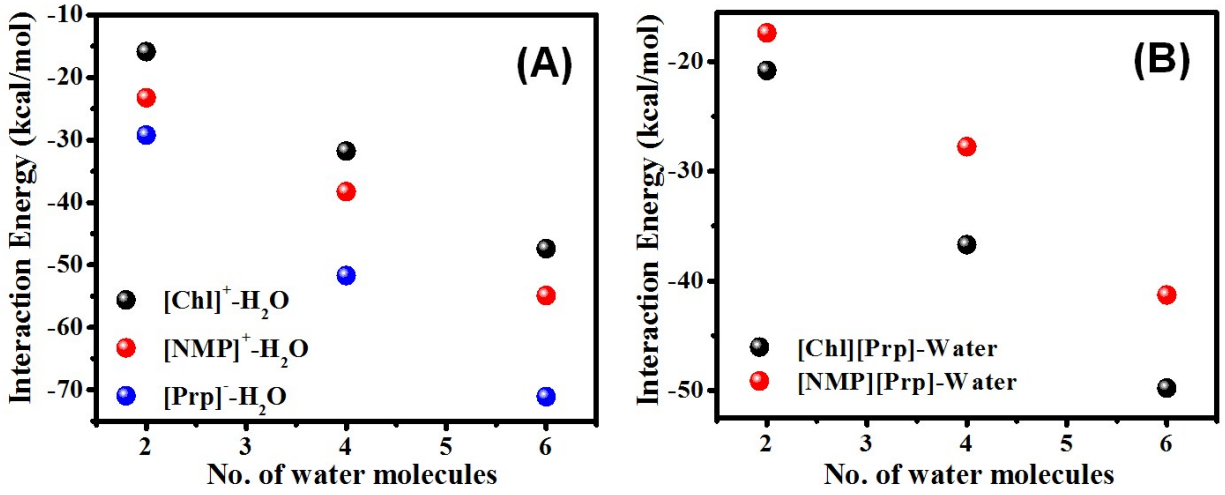

Figure S12. Interaction energy of individual ion-$(H_2O)_n$ **(A)** and IL-$(H_2O)_n$ **(B)** clusters.

Table S2. Calculated intramolecular bonds R_{O-H}, intermolecular bonds $R_{O-H}\cdots O$ (anion or water) and $R_O\cdots O-H$ (water) of the [Chl][Pro]-$(H_2O)_n$ complex and different number of water molecules at the HF/aug-cc-pVDZ level of theory.

System	CIP Cation_ R_{O-H} (Å)	CIP Cation-Anion_ $R_{O-H\cdots O}$ (Å)	CIP Anion-Water_ $R_{O\cdots H-O}$ (Å)	SIP Cation_ R_{O-H} (Å)	SIP Cation-Water_ $R_{O-H\cdots O}$ (Å)	SIP Anion-Water_ $R_{O\cdots H-O}$ (Å)
[Chl][Pro]	0.95680	1.91132	-	0.95680	-	-
[Chl][Pro]+2W	0.95546	1.92165	1.86182/ 1.83594	0.95445	1.93305	1.95585/ 1.81994
[Chl][Pro]+3W	0.95364	1.96183	1.91557/ 1.89341	0.94954	2.04409	1.89043/ 1.84748
[Chl][Pro]+4W	0.95357	1.96787	1.80379/ 1.93638	0.95117	1.95196	1.87477/ 1.78873
[Chl][Pro]+5W	0.95286	1.96450	1.76243/ 1.83475	0.95037	1.97068	1.87347/ 1.80677
[Chl][Pro]+6W	0.95376	1.93698	1.79766/ 1.85359	0.94929	2.03632	1.88406/ 1.80222
[Chl][Pro]+7W	0.95359	1.93123	1.76583/ 1.88829	0.95018	1.99894	1.89029/ 1.80605
[Chl][Pro]+8W	0.95316	1.95090	1.76558/ 1.79903	0.95005	1.99743	1.85778/ 1.82726

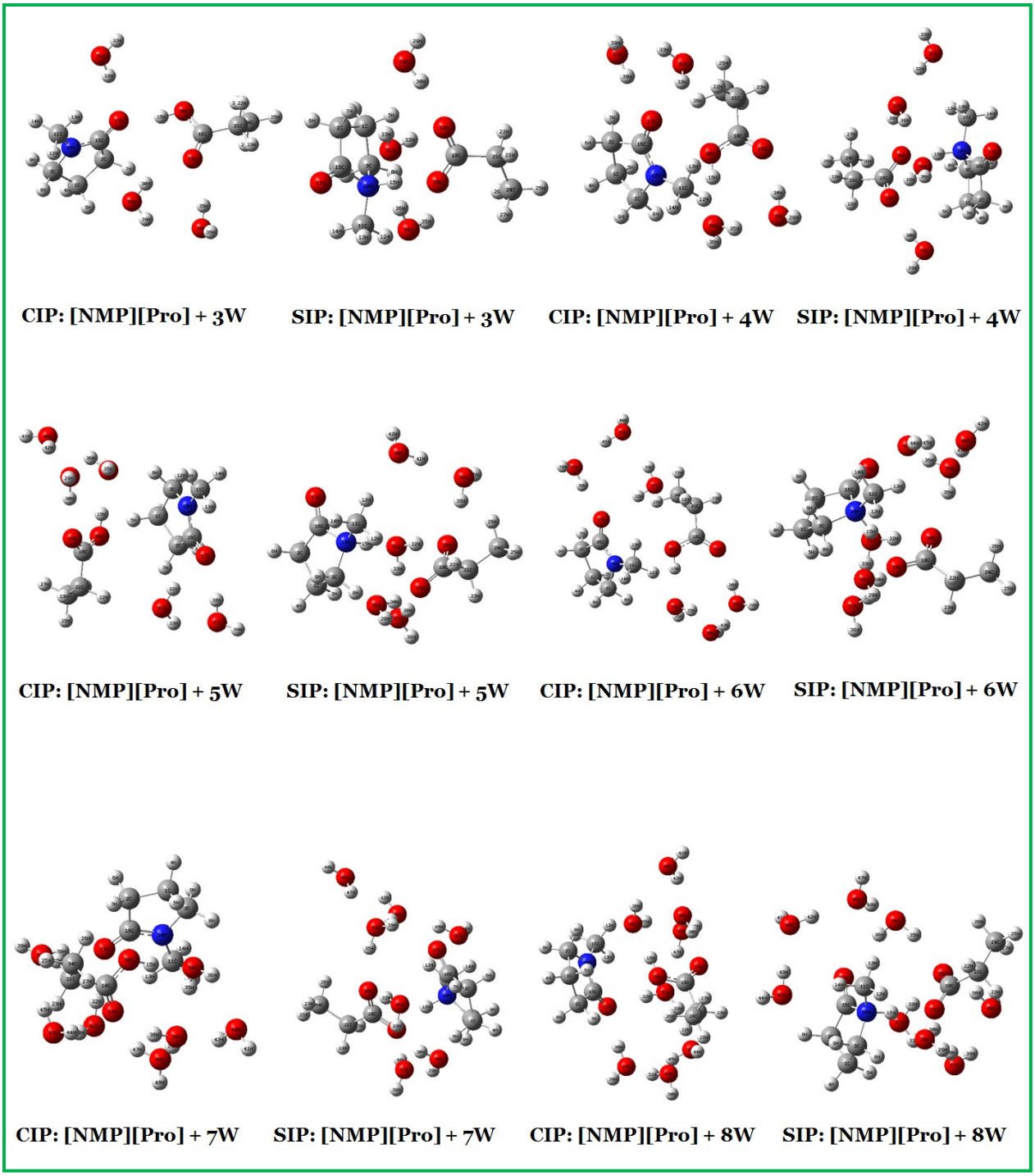

Figure S13. The most stable CIP and SIP configurations of the 1: n (n = 3-8) complexes including [NMP][Pro] ion-pair and different number of water molecules at HF/aug-cc-pVDZ level of theory.

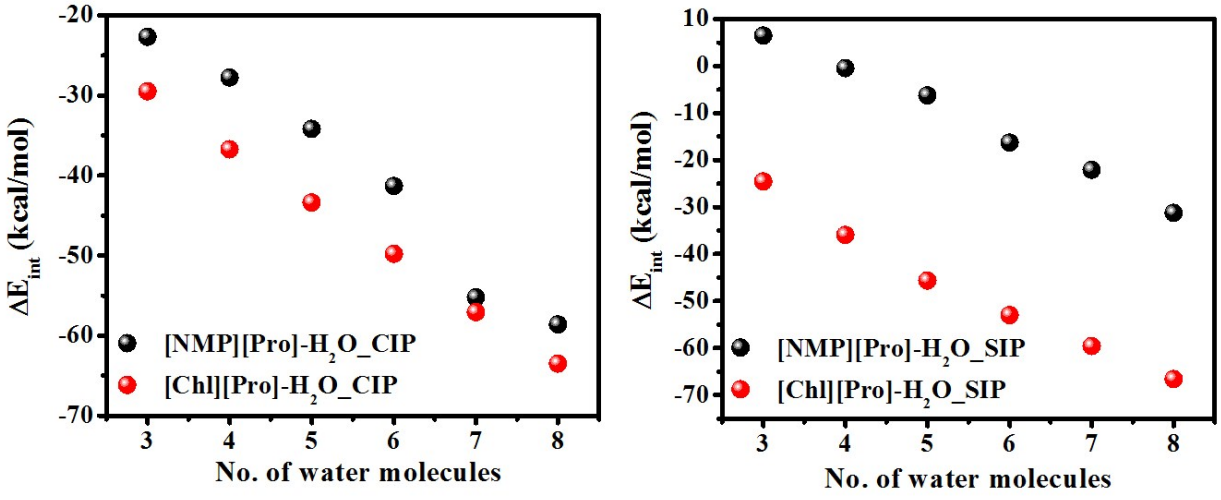

Figure S14. Comparative interaction energy of IL-$(H_2O)_n$ clusters at their CIP and SIP states.

Sec. 1. Purification of studied ILs and water: The purification of the studied ionic liquids was performed by the rotary evaporation followed by the vacuum to ensure the absence of unreacted initial materials, excess solvents and moisture. After this procedure, the purity of each IL was further checked by ^{1}H and ^{13}C NMR and confirmed to be >98 wt%. The ^{1}H and ^{13}C NMR of two ILs (Figures S1-S4) further confirmed the absence of any impurities in the synthesized ILs.

Further, it is well-known that the presence of excess water affect the viscosity of ILs substantially. In view of this, we have measured the viscosity of the neat ILs (290 and 2.8 mPa.s at 298 K for [Chl][Pro] and [NMP][Pro], respectively), which is found to be close to the reported value in literatures.[1,2] Double distilled was used for all measurements, which was passed across a reverse osmosis system, and further treated with a Milli-Q plus 185 water purification apparatus.

Sec. 2. Transition mechanisms from contact ion-pairs (CIPs) to solvent-shared ion-pairs (SIPs) in the IL-water mixtures: If the anion-cation interaction is sufficiently strong, contact ion pairs (CIPs) are the dominant structures in the IL-water mixtures. If the ion-solvent interaction is stronger, solvent-shared ion pairs (SIPs) prevail. Strong ion associations in pure or concentrated IL solutions resulted in the formation of an ion cage. The strong cation-anion association is rapidly weakened, when the water concentration is gradually increased, which resulted in the

slow disappearance of the cation-anion network structure (CIPs) and the formation of an ion-hydrated structure (SIPs). The cation-anion association network (CIPs) is believed to be completely replaced by the anion-water and/or cation-water network (SIPs) in an IL dilute-solutions. The reason for this phenomena is that water is a polar solvent and has a strong hydration capability. When the anion-water and/or cation-water H-bonding interactions in SIPs become much stronger than the cation-anion interaction, the CIPs are gradually replaced by a hydration shell in IL-water dilute solutions, i.e., SIPs.[3,4]

References

1. S. Panda, R. L. Gardas, *Fluid Phase Equilibr.* 2015, **386**, 65-74.

2. N. Muhammad, M. I. Hossain, Z. Man, M. El-Harbawi, M. A. Bustam, Y. A. Noaman, N. B. M. Alitheen, M. K. Ng, G. Hefter, C.-Y. Yin, *J. Chem. Eng. Data* 2012, **57**, 2191-2196.

3. P. Stange, K. Fumino, R. Ludwig, *Angew. Chem. Int. Ed.* 2013, **52**, 2990-2994.

4. K. Fumino, P. Stange, V. Fossog, R. Hempelmann, R. Ludwig, *Angew. Chem. Int. Ed.* 2013, **52**, 12439-12442.